JACS
JOURNAL OF THE AMERICAN CHEMICAL SOCIETY

Communication

pubs.acs.org/JACS

Titanosilicates with Strong Phase-Matched Second Harmonic Generation Responses

Tzu-Ling Chao,[†,§] Wen-Jung Chang,[†,§] Shu-Han Wen,[†] Yu-Qing Lin,[†] Bor-Chen Chang,[*,†] and Kwang-Hwa Lii[*,†,‡]

[†]Department of Chemistry, National Central University, Zhongli, Taiwan 320, R.O.C.

[‡]Institute of Chemistry, Academia Sinica, Taipei, Taiwan 115, R.O.C.

Supporting Information

ABSTRACT: The search for new and efficient nonlinear optical (NLO) materials has been an active research because of their technological importance in laser applications. Although a large number of frequency-doubling oxides, phosphates, borates, and fluoride-containing borates were found, no transition-metal silicate with useful NLO properties has been reported. We have now synthesized and grown crystals of two new titanosilicates, $Li_2K_4[(TiO)Si_4O_{12}]$ and $Li_2Rb_4[(TiO)Si_4O_{12}]$, by using a flux and supercritical hydrothermal method. Their unique 3D framework structures contain highly compressed TiO_5 square pyramids which are arranged one over the other to form infinite ···Ti−O··· Ti−O straight chains with alternating short and long Ti−O distances. These two materials meet the requirements for efficient second harmonic generation including lack of center of inversion symmetry, large susceptibility, phase matching, transmitting at wavelengths of interest, resistant to laser damage, and thermally stable. These attributes make them very attractive for frequency-doubling materials.

There has been a great interest in the search for new nonlinear optical (NLO) materials that exhibit efficient second harmonic generation (SHG).[1,2] Second-order NLO materials are used in optical switching, frequency conversion, and electro-optic applications. The requirements for NLO crystals for SHG include noncentrosymmetry, phase matching, larger effective second-order susceptibility value, higher laser-induced damage threshold, high transmittance at wavelengths of interest, and excellent chemical and thermal stabilities.[3] These requirements critically limit the candidate of crystals for NLO application. Organic NLO materials possess good optical nonlinearity, but their mechanical and thermal stabilities are poor and exhibit low laser-induced damage threshold. Most commercial NLO crystals are inorganics especially for high laser power use such as $LiNbO_3$, KH_2PO_4, $KTiOPO_4$, β-BaB_2O_4, LiB_3O_5, $KBe_2BO_3F_2$ (KBBF), and $Sr_2Be_2B_2O_7$.[2−5] A good number of SHG-active borate fluorides and fluorooxoborates have been reported.[6] KBBF was the sole NLO material that can generate SHG below 200 nm. Recently, a deep-UV borosilicate, a barium borate fluoride, and a beryllium-free lithium-aluminum-borate have also been synthesized.[7−9] In the quest for new efficient inorganic NLO crystals, we have now synthesized two silicate materials, $Li_2K_4[(TiO)Si_4O_{12}]$ (denoted as **1**) and $Li_2Rb_4[(TiO)Si_4O_{12}]$ (denoted as **2**) and determined their crystal structures. These two isostructural compounds are thermally stable, adopt a unique acentric crystal structure, transmitting at wavelengths of interest, and exhibit strong phase-matched SHG responses and high threshold to laser-induced damage. They are the first transition-metal silicates that exhibit efficient SHG.

These two titanosilicates were first synthesized by using mixtures of alkali metal fluorides as fluxes. Compound **1** was synthesized by heating a mixture of LiF (Sigma-Aldrich, 99%), KF (Merck, 99%), TiO_2 (Cerac, 99.9%), and SiO_2 (Alfa Aesar, 99.995%) (Li/K/Ti/Si molar ratio = 18/18/1/3) in a platinum crucible at 750 °C for 12 h. The crucible was cooled to 600 °C at 2 °C/h and then cooled to room temperature by turning off the power of the furnace. The flux was dissolved with hot water, and the solid product was separated by suction filtration, washed with water, rinsed with ethanol, and dried in a desiccator at ambient conditions. The reaction yielded colorless column crystals of **1** along with some undissolved LiF. A sample of **1** was obtained in a yield of 78% based on titanium via crystal picking. Colorless column crystals of **2** were obtained in a yield of 58% by heating a mixture of LiF, RbF (Alfa Aesar, 99%), TiO_2, and SiO_2 under the same reaction conditions. As shown in Figures S1 and S2, both samples were confirmed to be phase pure by powder X-ray diffraction using a Bruker D2 PHASER diffractometer with Cu Kα radiation. A qualitative X-ray fluorescence (XRF) analysis of several colorless column crystals of **1** and **2** using a Bruker S2 RANGER energy-dispersive XRF spectrometer confirmed the presence of K (or Rb), Ti, and Si and did not reveal any other element. Suitable crystals of **1** and **2** were selected for single-crystal X-ray diffraction analysis,[10] from which the chemical formulas were determined. A large crystal of **1** was grown using a top-seeded solution growth method.[11] The crystal was opaque in the area around the seed, which was probably because of flux inclusions. A transparent part of the crystal with each dimension ~5 mm was cut off with a diamond saw, polished, and used for laser-induced damage testing. The crystal is shown in Figure S3.

Compound **1** was also synthesized by a supercritical hydrothermal method. A reaction mixture of 19.6 mg of $LiOH·H_2O$, 0.469 mL of 5 M KOH(aq), 18.9 mg of TiO_2, and 56.7 mg of SiO_2 (molar ratio Li/K/Ti/Si = 2/10/1/4) in a 6.6 cm long

Received: May 24, 2016
Published: July 14, 2016

DOI: 10.1021/jacs.6b05327
J. Am. Chem. Soc. 2016, 138, 9061−9064

gold ampule, welded completely closed (inside diameter = 0.48 cm), was heated in a Tem-Pres high pressure vessel at 450 °C for 3 d. The degree of filling of the pressure vessel by water at rt was 55%, and the pressure was estimated to be 800 bar at the reaction temperature according to the $P-T$ diagram for pure water. The vessel was then cooled to 300 °C at 3.75 °C/h and quenched in air at rt by removing it from the tube furnace. The solid product was filtered, washed with water, rinsed with ethyl alcohol, and dried in a desiccator at rt. The reaction yielded colorless rod crystals of **1** as the only product, and the bulk product was pure as indicated powder X-ray diffraction. Attempts to prepare **2** by the supercritical hydrothermal method were unsuccessful. However, single-phase powder products of **1** and **2** could also be prepared quantitatively by heating a pressed pellet of a reaction mixture containing stoichiometric $LiOH{\cdot}H_2O$, K_2CO_3 (or $RbNO_3$), TiO_2, and SiO_2 (Li/K(or Rb)/Ti/Si molar ratio = 2/4/1/4) in a Pt crucible at 850 °C for 36 h with several intermittent grindings and slowly cooling to rt.

The thermal stability of **1** and **2** was investigated using a NETZSCH STA 449 F3 thermal analyzer on powder samples in a platinum crucible which were heated from rt to 1200 °C at 10 °C/min under flowing argon. The DSC and TGA curves are shown in Figures S4 and S5. The residues after the measurements were amorphous, as indicated by powder X-ray diffraction. A single crystal of **1** was heated at 700 °C in a platinum crucible in air for 5 h and then slowly cooled to rt. Diffraction data were collected on this crystal, and the structural analysis results did not reveal any significant change in the structure.

The UV−vis-NIR diffuse reflectance spectra were measured on polycrystalline samples of **1** and **2** at rt using a Hitachi U-4100 UV−vis-IR spectrometer equipped with an integrating sphere over the range of 200−2400 nm. $BaSO_4$ was used as a reference material. A Q-switched Nd:YAG laser (Spectra Physics INDI-40-10) operating at 1064 nm with pulse duration of 10 ns and repetition rate of 10 Hz was adopted as the light source for measuring the SHG efficiency.[12] For measuring the laser-induced damage threshold, the input 1064 nm laser power was tuned up to 100 mJ/pulse with a focused beam spot size of 1 mm in diameter.

The structure of **1** is formed from the following structural elements: one Li site, one K site, one TiO_5 square pyramid, and one SiO_4 tetrahedron. Both Li and K sites are ordered and fully occupied. The Li atom lies on a 2-fold axis, Ti and O(4) are on a 4-fold axis, and all the other atoms are in general positions. The TiO_5 polyhedron has one short titanyl bond (Ti−O(4) = 1.682(2) Å) and four longer Ti−O bonds (Ti−O(1) = 1.9760(9) Å) in the plane normal to the Ti−O(4) bond, forming a highly compressed square pyramid with a local symmetry of C_{4v}. The titanium atom is displaced 0.473 Å from the base center toward O(4). The titanyl bond in **1** is considerably shorter than those in $KTiOPO_4$ (1.718, 1.738 Å).[4] Square pyramidal $Ti(IV)O_5$ units with short titanyl bonds have also been observed in phosphates such as $Cs_2TiO(P_2O_7)$,[13] the silicate mineral fresnoite, $Ba_2TiOSi_2O_7$,[14,15] and the synthetic titanosilicate $Na_4Ti_2Si_8O_{22}{\cdot}2H_2O$.[16] The bond-valence sum (BVS) at the Ti site in **1**, calculated using the parameters R_0 = 1.815 Å and b = 0.37, is 4.02 valence units.[17] The Si atom is tetrahedrally coordinated by oxygen atoms with Si−O bond lengths ranging from 1.5924(8) to 1.664(1) Å. The BVS value at the Si site is 3.98. The BVS values for the O atoms are in the range of 1.89−2.12. The Li^+ cation is tetrahedrally coordinated by silicate oxygen atoms with d(Li(1)−O) = 1.934(3) Å (2×) and 1.955(3) Å (2×). The BVS value for Li(1) is 1.02. The coordination number of the K^+ cation is 9, and its BVS value is 1.00. Compound **2** is isostructural with **1**. The titanyl oxygen in **2** appears undersaturated, and its BVS value is 1.67 as compared with the corresponding value of 1.89 for **1**. The Ti−O(4) bond length in **2** is 1.666(4) Å, and the Ti atom is displaced 0.444 Å from the base center of the square pyramid.

As shown in Figure 1a, compound **1** has a 3D framework structure containing 12-ring channels along the c axis. The Li^+ and K^+ cations are located at different sites in the channels. The LiO_4 tetrahedra share opposite edges to form linear chains along the c axis. Chains of this kind are known in $BeCl_2$ and SiS_2 as well as in the anion of $K[FeS_2]$.[18] The structure of **1** consists of infinite chains of corner-sharing SiO_4 tetrahedra running parallel to the c-axis with a period of two tetrahedra. Each of the TiO_5 square pyramids shares its equatorial vertices with four silicate chains with the short titanyl Ti−O(4) group being unshared and directed in the same direction along the c-axis. The square pyramids are arranged one over the other so that the titanyl oxygen is directed toward the base of the adjacent square pyramid and infinite ···Ti−O···Ti−O straight chains with alternating short and long Ti−O distances (1.682, 3.318 Å for **1**; 1.666, 3.473 Å for **2**) are formed in the structure (Figures 1b and S6).

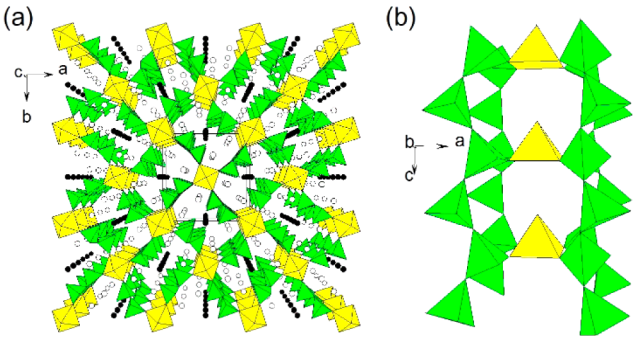

Figure 1. (a) Perspective view of the structure of **1** along the c axis. Key: Yellow square pyramid, TiO_5; green tetrahedron, SiO_4; solid circle, Li; open circle, K. (b) Section of the structure viewed along the b axis showing the connectivity between TiO_5 and silicate chains.

The DSC curves show endothermic peaks above 700 °C on heating but no exothermic peak on cooling (Figures S4 and S5). These results, combined with powder X-ray diffraction study of samples which were heated from 700 to 1000 °C, indicate that **1** and **2** melt incongruently at ∼900 and 920 °C, respectively. The occurrence of small endothermic peaks at ∼700 °C is very likely because of structural change. In situ high-temperature X-ray diffraction experiments are required to elucidate the details of the change. The mass losses between rt and 200 °C and above 950 °C are because of the loss of absorbed water and volatilization, respectively. Therefore, we conclude that these two compounds are thermally stable up to 700 °C. The UV−vis-NIR spectra of **1** and **2** are shown in Figure 2. In the range of 340−2400 nm, these two titanosilicates are transparent. The very weak peak at ∼1900 nm is ascribed to absorbed water. The diffuse reflectance spectra after Kubelka−Munk treatment are shown in the inset of Figure 2.[19] The calculated band gaps for **1** and **2** are 4.11 and 4.13 eV, respectively, by fixing the tangent line of the curve and the photon energy axis. These values are considerably larger than that of TiO_2 (3.31 eV). Since both compounds crystallize in a noncentrosymmetric space group, they are expected to be SHG-active. As shown in Figure 3, the SHG intensity of **1** and **2**

DOI: 10.1021/jacs.6b05327
J. Am. Chem. Soc. 2016, 138, 9061−9064

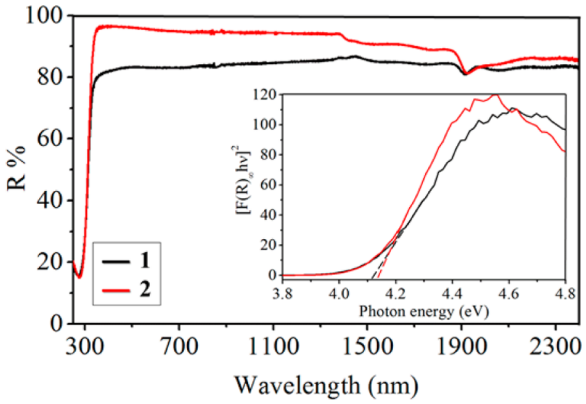

Figure 2. UV−vis-NIR diffuse reflectance spectra of polycrystalline **1** and **2**. The inset shows Kubelka−Munk transformed reflectance spectra of **1** and **2**.

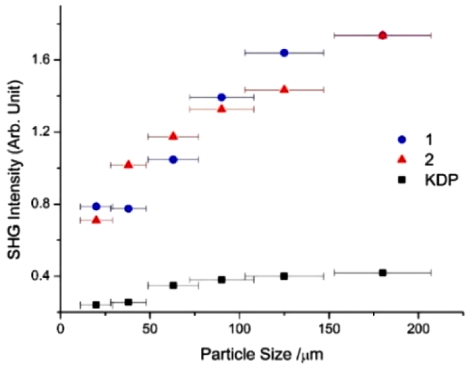

Figure 3. SHG intensity vs particle size curves for **1**, **2**, and KDP.

increases with particle size before it reaches the maximum independent of the particle size, indicating that both compounds are phase matchable.[20] The efficiencies of **1** and **2** are roughly 4.5 times stronger than that of KH_2PO_4 (KDP) in the 150−210 μm particle size range. Therefore, the two compounds belong to the class A category of SHG materials because they are phase matchable with large nonlinear coefficients.[21] Since a high laser-induced damage threshold value is crucial for an NLO crystal to be useful, laser damage threshold measurement was also performed. The input 1064 nm laser power was tuned up to 100 mJ/pulse and focused onto a crystal of **1** with each dimension ~5 mm and the beam spot size of 1 mm in diameter (~1.3 GW/cm^2 or 13 J/cm^2). A SHG green light was observed from the crystal, and the green light did not show any degradation under prolonged laser radiation (>3000 laser pulses). The laser-induced damage threshold value of **1** is >1.3 GW/cm^2, and this value can be compared with widely used SHG crystals such as β-BaB_2O_4 (>12 J/cm^2) and KDP (>18 J/cm^2).[22] The commercial versions of β-BaB_2O_4 and KDP have a laser-induced damage threshold value of 0.5 and 5.0 GW/cm^2, respectively.[23] Therefore, the title compounds are promising NLO materials for high-power applications.

One of the strategies to construct NLO materials is to incorporate noncentrosymmetric structural units such as strongly distorted octahedrally coordinated d^0 early transition metals into their crystal structures. However, the large deformation of the M−O polyhedron by itself does not produce an efficient SHG response, and the occurrence of a strong SHG response is most likely related to the orientation of the distorted polyhedra, as indicated by Gopalakrishnan et al. from studying the SHG responses of several Ti(IV) and Nb(V) borates, silicates, and phosphates.[24] Compounds **1** and **2** crystallize in the polar space group *P4nc* with the titanyl group being located on the 4-fold axis. Highly compressed TiO_5 square pyramids are aligned along the axis and directed in the same direction so that ···Ti−O···Ti−O chains are formed. This structural feature should have the largest influence on the SHG response. Although the synthetic titanosilicate $Na_4Ti_2Si_8O_{22}\cdot 4H_2O$ crystallizes in the acentric space group $P42_12$ and contains TiO_5 square pyramids, the geometric orientation of the polyhedra in the structure does not permit the formation of ···Ti−O···Ti−O chains, and its SHG response is rather weak (smaller than 5 times that of α-SiO_2).[16,24] The mineral fresnoite, $Ba_2TiOSi_2O_7$, crystallizes in the acentric space group *P4bm*, also contains TiO_5 square pyramids, and has the same structural features as those of the title compounds, namely infinite ···Ti−O···Ti−O straight chains with alternating short and long Ti−O distances. The SHG response of fresnoite with the particle sizes in the range of 150−200 μm was reported to be ~1250 times that of α-SiO_2.[24] Zhao et al. reported that in the same particle size range, the SHG response of fresnoite is ~3.5 times that of KDP,[25] which is a little smaller than those of **1** and **2**. However, the birefringence of fresnoite in the visible region does not allow phase-matched SHG.[26] Therefore, we can conclude that the polar structure of **1** and **2** that results from the alignment of highly compressed TiO_5 square pyramids is responsible for the large SHG intensity. As for the contribution to SHG of other building units in the structure, the rigid silicate groups and hard Li^+ cation should contribute little to the SHG response. The Rb^+ cation is expected to have a larger contribution than K^+ because the former is more readily polarized.

Efficient inorganic SHG materials for Nd:YAG lasers were found in oxides, borates, phosphates, and a borosilicate. $Li_2K_4[(TiO)Si_4O_{12}]$ and $Li_2Rb_4[(TiO)Si_4O_{12}]$ adopt a unique structure which allows constructive addition of individual Ti−O bond polarizabilities and are the first examples of transition-metal silicates with useful NLO properties such as large phase-matched SHG responses and high threshold to laser-induced damage. They are very promising materials for frequency doubling. This work opens a new dimension to the research on NLO materials. The germanate analogue of **1** with a large SHG response has also been synthesized and structurally characterized.[27] Further research to grow large high-quality crystals of these two titanosilicates for detailed NLO property studies and to synthesize new NLO silicate and germanate materials is in progress.

■ ASSOCIATED CONTENT

Supporting Information

The Supporting Information is available free of charge on the ACS Publications website at DOI: 10.1021/jacs.6b05327.

Crystal data in CIF format, X-ray powder pattern, photo of a crystal, and TGA/DSC data (PDF)
(TXT)
(TXT)

■ AUTHOR INFORMATION

Corresponding Authors

*liikh@cc.ncu.edu.tw
*bchang@ncu.edu.tw

Author Contributions

§These authors contributed equally.

DOI: 10.1021/jacs.6b05327
J. Am. Chem. Soc. 2016, 138, 9061−9064

Notes

The authors declare no competing financial interest.

■ ACKNOWLEDGMENTS

This research is financially supported by the Ministry of Science and Technology of Taiwan under grant nos. 104-2113-M-008-001-MY3 (K.-H.L.) and 104-2113-M-008-004 (B.-C.C.).

■ REFERENCES

(1) Eaton, D. F. *Science* **1991**, *253*, 281−287.
(2) Ye, N.; Tu, C.; Long, X.; Hong, M. *Cryst. Growth Des.* **2010**, *10*, 4672−4681.
(3) He, G. S.; Liu, S. H. *Physics of Nonlinear Optics*; World Scientific: Singapore, 1999; Ch. 3.
(4) Stucky, G. D.; Phillips, M. L. F.; Gier, T. E. *Chem. Mater.* **1989**, *1*, 492−509.
(5) Chen, C.; Wang, Y.; Wu, B.; Wu, K.; Zeng, W.; Yu, L. *Nature* **1995**, *373*, 322−324.
(6) In *Photonic and Electronic Properties of Fluoride Materials*; Tressaud, A., Poeppelmeier, K., Eds.; Elsevier: Amsterdam, 2016; Chpts 6 and 15.
(7) Wu, H.; Yu, H.; Pan, S.; Huang, Z.; Yang, Z.; Su, X.; Poeppelmeier, K. R. *Angew. Chem., Int. Ed.* **2013**, *52*, 3406−3410.
(8) Wu, H.; Yu, H.; Yang, Z.; Hou, X.; Su, X.; Pan, S.; Poeppelmeier, K. R.; Rondinelli, J. M. *J. Am. Chem. Soc.* **2013**, *135*, 4215−4218.
(9) Zhao, S.; Kang, L.; Shen, Y.; Wang, X.; Asghar, M. A.; Lin, Z.; Xu, Y.; Zeng, S.; Hong, M.; Luo, J. *J. Am. Chem. Soc.* **2016**, *138*, 2961−2964.
(10) For single-crystal diffraction analysis, data were collected on colorless column crystals of **1** and **2** at 296 K using a Bruker Kappa APEX II CCD diffractometer with monochromated Mo Kα (λ = 0.71073 Å) radiation. The crystallographic data and structural refinement results are summarized as follows: Compound **1**: tetragonal, space group *P4nc* (no. 104), M_r = 538.54, a = 11.331(1) Å, c = 5.0001(1) Å, V = 642.0(1) Å^3, Z = 2, ρ_{calcd} = 2.786 g cm^{-3}, μ(Mo Kα) = 24.1 cm^{-1}, crystal size = 0.06 × 0.08 × 0.21 mm^3, 12850 reflections measured, 793 independent reflections with R_{int} = 0.0194, $R1$ = 0.0106 and $wR2$ = 0.0356 for 791 reflections with $I > 2\sigma(I)$ and 58 parameters. The flack parameter is 0.04(2). Compound **2**: the same as those in **1** except M_r = 724.02, a = 11.5037(5) Å, c = 5.1396(3) Å, V = 680.15(6) Å^3, ρ_{calcd} = 3.535 g cm^{-3}, μ(Mo Kα) = 152.7 cm^{-1}, crystal size = 0.05 × 0.05 × 0.26 mm^3, 7676 reflections measured, 736 independent reflections with R_{int} = 0.0242, $R1$ = 0.0179 and $wR2$ = 0.0399 for 698 reflections with $I > 2\sigma(I)$. The flack parameter is 0.01(1). Crystallographic data and selected bond lengths are given in Tables S1 and S2.
(11) Several high-quality crystals of **1** were selected as seeds to grow large-sized single crystals. A seed crystal was attached with a Pt wire to a Pt rod and slightly introduced into the surface of the melt at 2 °C above the saturation temperature. The melt was cooled at a rate of 0.1 °C/h until a large crystal was obtained. The crystal was pulled out of the melt and then cooled to rt at a rate of 20 °C/h. Our equipment does not have a pulling and rotating system.
(12) For SHG measurements, the 1064 nm laser beam was focused onto the sample capillary and the scattered SHG signal at 532 nm was collected and imaged onto a monochromator (Acton Research Corp. SP2300i) attached with a photomultiplier tube (EMI 9658QB) as the detector. The signal waveform was recorded in a digital oscilloscope (LeCroy WR64xi), which is linked with a personal computer. The SHG spectra at 532 nm were recorded by scanning the monochromatic wavelength. Polycrystalline samples were ground and sieved into several specific particle size ranges (20, 38, 63, 90, 125, and 180 μm) and were contained in a quartz glass capillary tube in 1 mm inner diameter. The sieved KDP powders were used as a reference. To eliminate the intensity fluctuation caused by powder packing density, the scattered signal of 1064 nm was also recorded for SHG signal normalization. In the SHG efficiency measurements, the input 1064 nm laser beam was limited to be <2 mJ/pulse to prevent signal saturation. The SHG efficiencies of **1**, **2**, and KDP were acquired for each particle size range.
(13) Daidouh, A.; Veiga, M. L.; Pico, C. *Solid State Ionics* **1997**, *104*, 285−294.
(14) Moore, P. B.; Louisnathan, J. *Science* **1967**, *156*, 1361−1362.
(15) Masse, R.; Grenier, J.-C.; Durif, A. *Bull. Soc. Fr. Mineral. Cristallogr.* **1967**, *90*, 20−23.
(16) Roberts, M. A.; Sankar, G.; Thomas, J. M.; Jones, R. H.; Du, H.; Chen, J.; Pang, W.; Xu, R. *Nature* **1996**, *381*, 401−404.
(17) Brown, I. D.; Altermatt, D. *Acta Crystallogr., Sect. B: Struct. Sci.* **1985**, *41*, 244−247.
(18) Müller, U. *Inorganic Structural Chemistry*; John Wiley & Sons: Chichester, 1992; Chpt. 15.
(19) Kubelka, P.; Munk, F. *Z. Technol. Phys.* **1931**, *12*, 593−601.
(20) Dougherty, J. P.; Kurtz, S. K. *J. Appl. Crystallogr.* **1976**, *9*, 145−158.
(21) Kurtz, S. K.; Perry, T. T. *J. Appl. Phys.* **1968**, *39*, 3798−3813.
(22) Ristau, D., Ed. *Laser-Induced Damage Threshold in Optical Materials*; CRC Press: Boca Raton, FL, 2014; pp 295−297.
(23) The damage threshold values of commercial β-BaB_2O_4 and KDP are available from the website of CASTECH Inc. http://www.castech.com/, accessed July 10, 2016.
(24) Gopalakrishnan, J.; Ramesha, K.; Kasthuri Rangan, K.; Pandey, S. *J. Solid State Chem.* **1999**, *148*, 75−80.
(25) Zhao, W.; Zhang, F.; Liu, J.; Hao, B.; Pan, S.; Zhang, F. *J. Cryst. Growth* **2015**, *413*, 46−50.
(26) Bechthold, P. S.; Haussuhl, S.; Michael, E.; Eckstein, J.; Recker, K.; Wallrafen, F. *Phys. Lett. A* **1978**, *65*, 453−454.
(27) Crystal data for $Li_2K_4[(TiO)Ge_4O_{12}]$: tetragonal, space group *P4nc* (no. 104), M_r = 716.54, a = 11.590(2) Å, c = 5.1672(9) Å, V = 694.0(2) Å^3, Z = 2, crystal size = 0.024 × 0.022 × 0.011 mm^3, $R1$ = 0.0310 and $wR2$ = 0.0485 for 788 reflections with $I > 2\sigma(I)$ and 58 parameters. The flack parameter is 0.05(2). This germanate is isostructural with compound **1** and its SHG efficiency is ∼4.2 times stronger than that of KDP in the 150−210 particle size range.

DOI: 10.1021/jacs.6b05327
J. Am. Chem. Soc. 2016, 138, 9061−9064